Neurol Ther (2026) 15:2153–2166
https://doi.org/10.1007/s40120-026-00965-5

BRIEF REPORT

Inter-assay and Inter-site Performance of Alpha-Synuclein Seed Amplification Assays in Synucleinopathies: A Multicenter 2 × 2 Protocol Comparison

Roger Plaza-Clar · Maximilian Weber · Vaibhavi Kadam · Christian Deuschle · Yihua Ma · Carly M. Farris · Luis Concha-Marambio · David Mengel · Marcello Rossi · Angela Mammana · Piero Parchi · Matthis Synofzik · Kathrin Brockmann · Thomas Gasser

Received: March 4, 2026 / Accepted: May 11, 2026 / Published online: May 27, 2026

ABSTRACT

Introduction: The α-synuclein seed amplification assay (synSAA) is a biomarker test for synucleinopathies. Different synSAA conditions have different properties, and some of these conditions enable differentiation between diseases associated with Lewy bodies versus those associated with glial inclusions. Direct cross-assay and inter-site synSAA comparisons evaluating these features remain limited.

Methods: Two synSAA conditions (identified here as sodium phosphate buffer (SPB) and piperazine-*N*,*N*′-bis(2-ethanesulfonic acid) (PIPES) SAA conditions) were tested in a controlled 2 × 2 design, each performed at two independent laboratories. Cerebrospinal fluid (CSF) from 60 participants was analyzed, comprising 29 multiple system atrophy (MSA) samples and 31 additional CSF samples including 16 Parkinson's disease/dementia with Lewy bodies (PD/DLB) cases previously screened using SPB-SAA conditions, and 15 neurology ward controls, which were used as analytical controls.

Results: Inter-site concordance was high for SPB-SAA (100%) and PIPES-SAA (95%, 0.913 Fleiss' kappa). Compared to clinical diagnosis, sensitivity for detecting synSAA+ MSA cases was 75.0% for PIPES-SAA_A and 81.4% for PIPES-SAA_C, with specificities of 76.9% and 92.3%, respectively. SPB-SAA did not detect MSA at either of the two sites and showed 100% specificity. Inter-assay concordance was high for PD/DLB (88%) and controls (86%), but low for MSA (31%), reflecting the different sensitivity in MSA cases. The overall inter-assay concordance yielded a Fleiss' kappa of 0.23.

Conclusion: Both synSAA conditions exhibit high reproducibility and replicability across

Roger Plaza-Clar, Maximilian Weber, and Vaibhavi Kadam contributed equally to this work and share first authorship.

Supplementary Information The online version contains supplementary material available at https://doi.org/10.1007/s40120-026-00965-5.

R. Plaza-Clar (✉) · M. Weber · V. Kadam · C. Deuschle · D. Mengel · M. Synofzik · K. Brockmann · T. Gasser
Department of Neurodegeneration and Hertie-Institute for Clinical Brain Research, University of Tuebingen, Tuebingen, Germany
e-mail: rogerplazac@gmail.com

R. Plaza-Clar · M. Weber · V. Kadam · C. Deuschle · D. Mengel · M. Synofzik · K. Brockmann · T. Gasser
German Center for Neurodegenerative Diseases, Tuebingen, Germany

Y. Ma · C. M. Farris · L. Concha-Marambio
Amprion, San Diego, CA, USA

M. Rossi · A. Mammana · P. Parchi
IRCCS Istituto delle Scienze Neurologiche di Bologna, Bologna, Italy

P. Parchi
Department of Biomedical and Neuromotor Sciences, University of Bologna, Bologna, Italy

laboratories yet differ in their diagnostic profiles: PIPES-SAA conditions enable detection of synuclein seeds in MSA, while SPB-SAA conditions showed high specificity for PD/DLB but not detect synuclein seeds in MSA. These findings support context-dependent assay selection and underscore the need for larger multicenter validation of analytical tools intended for clinical use.

Keywords: α-Synuclein; Seed amplification assays; Synucleinopathies; Parkinson's disease; Dementia with Lewy bodies; Multiple systems atrophy

Key Summary Points

Why carry out this study?

α-Synuclein seed amplification assays (synSAAs) enable ultrasensitive detection of misfolded α-synuclein aggregates in cerebrospinal fluid (CSF), offering clinical biomarker applications in synucleinopathies.

Direct inter-assay and inter-site comparisons of optimized synSAAs, particularly for multiple systems atrophy (MSA), remain limited despite increasing clinical use.

What was learned from the study?

In this multicenter 2 × 2 comparison, two synSAA conditions demonstrated high inter-site reproducibility, confirming their technical robustness across laboratories.

Clinically, assay selection should align with the diagnostic goal: confirming Parkinson's disease/dementia with Lewy bodies (PD/DLB) with sodium phosphate buffer SAA (SPB-SAA) or exploring broader synucleinopathy profiles with piperazine-*N*,*N*′-bis(2-ethanesulfonic acid SAA (PIPES-SAA).

INTRODUCTION

Synucleinopathies, including Parkinson's disease (PD), dementia with Lewy bodies (DLB), and multiple system atrophy (MSA), are neurodegenerative diseases characterized by the accumulation of pathologically misfolded alpha-synuclein (αSyn) protein aggregates [1]. Although the differential diagnosis of parkinsonism encompasses a broader spectrum of disorders, including tauopathies such as progressive supranuclear palsy (PSP) and corticobasal degeneration (CBD) [2], PD, DLB, and MSA are unified by αSyn pathology and are therefore the primary targets of synSAA-based diagnostics. While in PD and DLB (PD/DLB) αSyn pathology is primarily found in neurons forming Lewy bodies and Lewy neurites, in MSA it accumulates in oligodendrocytes, forming glial cytoplasmatic inclusions (GCIs) [3]. Misfolded synuclein aggregates extracted from PD/DLB cases have different structure and features, both in vitro and in vivo, than misfolded synuclein from MSA cases [4–7].

Although these disorders can share overlapping clinical features, they differ in symptom progression, prognosis, and therapeutic response. Traditionally, diagnosis has relied primarily on clinical criteria, often resulting in diagnostic uncertainty, particularly in early stages [8]. For many years, the lack of reliable, disease-specific biomarkers has impeded accurate differential diagnosis. The development of biological biomarkers, such as the detection of pathological misfolded αSyn through seed amplification assays (synSAA), sought to aid in diagnosis [9].

SAAs were first developed as diagnostic tools for the detection of prions [10, 11], and the technology has since been adapted to detect pathological misfolded αSyn in brain extracts, cerebrospinal fluid (CSF), and other biomatrices [12, 13]. Many synSAA experimental conditions have been reported, and a body of evidence demonstrates synSAAs can identify individuals with underlying synuclein pathology, differentiating PD/DLB from control and mimics [14–16]. Moreover, it has been recently shown that synSAAs can discriminate between

type 1 synuclein seeds associated with PD/DLB and type 2 synuclein seeds associated with MSA [17–19].

In this multicenter study, we evaluate the inter-assay and inter-site reproducibility of two synSAA protocols within a controlled 2 × 2 design. Two sites used the synSAA protocol from Rossi and colleagues [14], sodium phosphate buffer-SAA (SPB-SAA) herein; and two sites used the synSAA protocol from Ma, Farris, and colleagues [18], PIPES-SAA herein. In addition to evaluating technical reproducibility by using a shared cohort of CSF samples, we specifically compared the protocols' ability to detect synuclein seeding activity in clinically diagnosed MSA and to capture type 2 seeding profiles, which is a feature of the PIPES-SAA conditions. This work provides new insights into the diagnostic profiles, reproducibility, and complementarity of synSAAs across protocols and laboratories.

METHODS

Study Population

Between 2006 and 2020, 11 patients with PD, 5 patients with DLB, 29 patients with MSA, and 15 controls were recruited for lumbar puncture at the University Hospital of Tuebingen. PD was diagnosed following the UK Brain Bank Society criteria [20], DLB was diagnosed following the fourth consensus report of the DLB Consortium [21], MSA was clinically diagnosed following the 2008 Second Consensus Statement (MSA-SCS08) [22]. Importantly, all patients with MSA were diagnosed at two or more clinical visits. Patient characteristics are summarized in Table 1. The control group consisted of patients without neurodegenerative disease diagnoses from the neurological ward. Their individual diagnoses are provided in supplementary Table S1.

Spinal tap was performed between 9.00 am and 1.00 pm. Samples were centrifuged at 2000×*g* for 10 min at room temperature within 60 min and frozen at −80 °C within 90 min after collection. Samples with abnormal routine CSF diagnostics (erythrocytes > 1/µL, white blood cell count > 5 cells/µL, immunoglobulin subtype G index > 0.7) were excluded [23].

Table 1 Patient characteristics by diagnostic group

	PD/DLB*	MSA	Controls
Number	16	29	15
Sex (m/f)	8/8	17/12	5/10
Age at visit	69.63 ± 7.37	61.03 ± 7.26	60.4 ± 20.03
Age at onset	66.38 ± 7.82	57.07 ± 7.91	NA
Disease duration	3.25 ± 1.53	3.97 ± 2.73	NA

Data depicted as mean ± standard deviation

PD Parkinson's disease, *DLB* dementia with Lewy bodies, *MSA* multiple systems atrophy, *m* male, *f* Female, *NA* data not available

*Cohort specially selected for methodological purposes

The PD/DLB subgroup was selected for methodological reasons to assess the technical reproducibility of the assays. Only the 11 patients with PD and 5 patients with DLB were prescreened for synSAA as part of a larger cohort previously published in Brockmann et al., 2021 [24] using the SPB-SAA conditions. From this pre-screening, we deliberately enriched the PD/DLB subgroup with individuals lacking detectable αSyn seeding activity to challenge assay sensitivity. In the previous publication, only 9 of the selected 16 PD/DLB samples were synSAA+, while the overall rate of synSAA+ for the PD/DLB group was 85% [18, 24]. Consequently, this methodological enrichment introduces a bias, as this subset does not reflect the expected detection rates in clinical PD/DLB population. Throughout the manuscript, the PD/DLB subgroup is marked with an asterisk (*) to denote its methodological nature. In contrast, the MSA and control groups were selected with a diagnostic rationale, enabling the evaluation of assay sensitivity, and technical reproducibility under clinically relevant conditions. Most of these samples, including the MSA and control groups, were also analyzed by Amprion (using the PIPES-SAA conditions) and reported as the "EKUT" cohort in *The Lancet Neurology* [18].

The study was approved by the Ethics Committee of the University of Tuebingen (353/2022BO2). All participants gave written informed consent for participation in the study and for the use and publication of their anonymized data. This study was conducted in accordance with the principles of the Declaration of Helsinki.

Study Structure and Sample Handling

CSF sample testing was performed at three sites: University of Tuebingen (site A), Institute of Neurological Science of Bologna (site B), and Amprion R&D (site C). Sites A and B used the SPB-SAA protocol (tests deemed SPB-SAA_A and SPB-SAA_B) and sites A and C used the PIPES-SAA (tests deemed PIPES-SAA_A and PIPES-SAA_C). CSF samples (500 µL) were redistributed on ice into 2 × 100-µL aliquots for the SPB-SAA protocol and 2 × 150-µL aliquots for the PIPES-SAA protocol. These aliquots were deidentified, stored at − 80 °C, and shipped to each site for testing. All synSAA analyses were carried out blindly with respect to disease status. Unblinding and data analysis were performed after all results had been obtained.

α-Synuclein Seed Amplification Assays

SPB-SAA protocol. Testing was performed at sites A and B according to Rossi et al., 2020. Briefly, 15 µL of CSF was mixed with 85 µL of reaction buffer in each well of a black, clear-bottom 96-well plate (Thermo Fischer Scientific), each containing six 0.8-mm silica beads (OPS Diagnostics). The reaction buffer consisted of 40 mM phosphate buffer (pH 8.0), 0.0015% SDS, 10 µM Thioflavin T, 170 mM NaCl, and 0.1 mg/ml recombinant monomeric αSyn previously filtered through a 100-kDa MWCO centrifugal filter. Recombinant monomeric αSyn was produced as previously described [14] at site B and was used at sites A and B. Plates were then incubated at 42 °C in a FLUOstar Omega plate reader (BMG Labtech) with alternating cycles of 1 min double orbital shaking at 400 rpm and 1 min rest. Fluorescence was measured every 45 min using a 448-nm excitation and 482-nm emission filter. Four technical replicates per sample were included in each assay plate. Two positive and two negative controls (each with four replicates) were also included on every plate. Fluorescence values were normalized as a percentage of the maximum signal of each plate. A replicate was considered synSAA+ if its fluorescence exceeded a defined threshold within the first 40 h. The threshold was calculated as the mean fluorescence of previous negative controls during the first 10 h of measurement, plus 40 standard deviations. A sample was considered synSAA+ if at least two replicates were positive and was categorized as "synSAA+ type 1". A sample was considered synSAA− if none of the replicates were positive. At site A, samples with only one positive replicate were retested. Classification was based on the repeat run only, if two or more replicates were positive upon retesting, the sample was considered synSAA+. Otherwise, it was considered synSAA−. At site B, as a result of limited material availability, retesting was not possible, and samples with a single positive replicate were assigned an "inconclusive" status.

PIPES-SAA protocol. Testing was performed at sites A and C according to Ma, Farris, et al., 2024. Briefly, 40 µL of CSF was mixed with 60 µL of reaction buffer in each well of a black, clear-bottom 96-well microplate (Greiner), each containing two 1/8" silicon nitride beads (Tsubaki Nakashima). The reaction buffer consisted of 100 mM PIPES buffer (pH 6.5), 0.1% Sarkosyl (Milipore Sigma), 10 µL of Thioflavin T, 0.44 M NaCl, and 0.3 mg/mL of unfiltered recombinant monomeric αSyn (Amprion, #S2020). Plates were incubated at 42 °C in a FLUOstar Omega plate reader (BMG Labtech) for 24 h. Each amplification cycle consisted of 1 min of orbital shaking at 800 rpm followed by 14 min of rest. Fluorescence was measured using 440/10-nm excitation and 490/10-nm emission filters. The plate readers at both sites were previously calibrated using Atto425 fluorescent dye as standard [18]. Each sample was tested in three technical replicates. For each replicate, the maximum fluorescence intensity (Fmax) was used for classification: values ≥ 45,000 RFU were classified as type 1 replicates, values between 3000 and 44,999 RFU were classified as type 2 replicates, and

values < 3000 RFU were considered synSAA–. CSF samples with three type 1 replicates were considered synSAA+ with type 1 synuclein seeds (predominantly seen in individuals with PD/DLB clinical diagnosis) and categorized as "synSAA+ type 1". Samples with two or three replicates with type 2 replicates were considered synSAA+ with type 2 synuclein seeds (predominantly seen in individuals with MSA clinical diagnosis) and categorized as "synSAA+ type 2". Samples with two or three negative replicates were considered synSAA–. Samples with two type 1 replicates and one type 2 replicates were considered synSAA+ of underdetermined seed type, and other combinations were considered inconclusive and were assigned an "inconclusive" status. Retest is recommended for inconclusive and synSAA+ undetermined samples. However, no CSF was available for retest for these assay conditions [18]. Analysis of SAA fluorescence data was conducted using MARS Omega data analysis software 4.00 R2 (BMG Labtech).

A comparison of both SAA protocols can be found in Table 2.

Statistical Analysis

GraphPad Prism 9.5 and Python 3.10.16 (statsmodels 0.14.4, motplotlib 3.5.3) were used for statistical analysis and data visualization. Descriptive statistics for patient characteristics, as well as diagnostic sensitivity for MSA detection, were calculated in GraphPad Prism, excluding individuals with inconclusive classification. Sensitivities were plotted with 95% confidence intervals, computed using the Clopper-Pearson exact method, and represented as error bars in the corresponding figure.

Inter-assay and inter-site concordance were assessed as the percentage of concordant classifications overall, and within each diagnostic subgroup. To quantify agreement beyond chance, Fleiss' kappa coefficients and associated p values were computed using Python with the statsmodels.stats.inter_rater module.

Table 2 Comparison of experimental conditions across synSAA protocols

	SPB-SAA	PIPES-SAA
Monomeric αSyn	0.1 mg/ml filtered	0.3 mg/ml unfiltered
Reaction volume	100 µL	100 µL
CSF	15% v/v	40% v/v
Reaction buffer composition	40 mM phosphate (pH 8) 0.0015% SDS 170 mM NaCl 10 µM ThT	100 mM PIPES (pH 6.5) 0.1% Sarkosyl 0.44 M NaCl 10 µM ThT
Beads	Six 0.8 mm silica	Two 1/8″ silicon nitride
Temperature	42 °C	42 °C
Shaking	Double orbital 400 rpm for 1 min, 1 min rest	Orbital 800 rpm for 1 min, 14 min rest
Total assay duration	40 h	24 h

Summary of the main protocol parameters for the SPB-SAA and PIPES-SAA applied in this study

αSyn alpha-synuclein, *CSF* cerebrospinal fluid, *SDS* sodium dodecyl sulfate, *ThT* Thioflavin T, *PIPES* piperazine-*N*,*N*′-bis(2-ethanesulfonic acid), *NaCl* sodium chloride, *SPB-SAA* sodium phosphate buffer seed amplification assay, *PIPES-SAA* piperazine-*N*,*N*′-bis(2-ethanesulfonic acid) seed amplification assay

Negative kappa values indicate less agreement than expected by chance.

No correction for multiple comparisons was applied. A p value < 0.05 was considered statistically significant for all analyses.

RESULTS

Sixty participants were included in the study: 16 patients with PD or DLB (PD/DLB*), 29 patients with MSA, and 15 controls. The PD/DLB* subgroup was specifically selected as a methodological cohort, as described in the Methods section. Thus, no diagnostic performance was assessed for this subgroup. On the other hand, patients with MSA and controls were selected for diagnostic evaluation purposes.

The analyses were focused on assay classification outcomes, their distribution, inter-assay concordance, and diagnostic sensitivity and specificity (excluding the PD/DLB* subgroup).

Classification Outcomes per Assay and Subgroup

We first examined the classification outcomes assigned by each assay across the three diagnostic subgroups visualized in Figs. 1, 2, and 3, corresponding to PD/DLB*, MSA, and control participants, respectively.

For clarity, assays are denoted by site and protocol: PIPES-SAA_A and PIPES-SAA_C refer to synSAA performed at sites A (University Hospital of Tuebingen) and C (Amprion R&D) using the PIPES-SAA protocol, respectively, while SPB-SAA_A and SPB-SAA_B refer to synSAA performed at sites A and B (Institute of Neurological Science of Bologna) using the SPB-SAA protocol.

In the PD/DLB* subgroup, SPB-SAA_A and SPB-SAA_B classified 9 out of 16 cases as synSAA+ and the remaining as non-seeders, demonstrating identical classification performance after remeasuring two inconclusive cases in the SPB-SAA_A. PIPES-SAA_A and PIPES-SAA_C also classified 9 patients as synSAA+ and the remaining were categorized as synSAA–, demonstrating

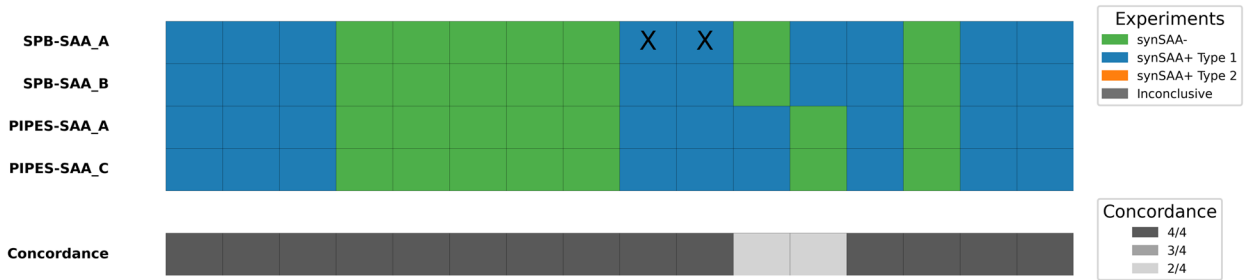

	synSAA-	synSAA+ Type 1	synSAA+ Type 2	Inconclusive
SPB-SAA_A	7	9	0	0
SPB-SAA_B	7	9	0	0
PIPES-SAA_A	7	9	0	0
PIPES-SAA_C	7	9	0	0

Fig. 1 Classification outcomes per assay of the Parkinson's disease/dementia with Lewy bodies (PD/DLB*) subgroup. Graph showing the diagnostic classification assigned by each assay (SPB-SAA_A, SPB-SAA _B, PIPES-SAA_A, PIPES-SAA _C) for each individual patient (columns), where SPB-SAA refers to sodium phosphate buffer seed amplification assay and PIPES-SAA refers to piperazine-*N*,*N*′-bis(2-ethanesulfonic acid) seed amplification assay. Colors represent the classification outcome per assay: synSAA+ type 1, synSAA+ type 2, synSAA–, or inconclusive. In SPB-SAA_A, an "X" marks the samples that required retesting due to an initial inconclusive result. Lower row shows the concordance rate between sites (number of concordant results per 4 assays). At the bottom, a summary table reports the total number of patients classified into each category by assay

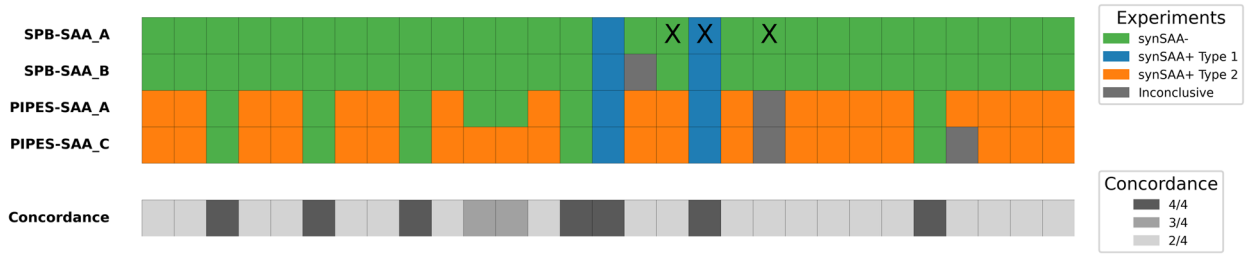

	synSAA-	synSAA+ Type 1	synSAA+ Type 2	Inconclusive
SPB-SAA_A	27	2	0	0
SPB-SAA_B	26	2	0	1
PIPES-SAA_A	7	2	19	1
PIPES-SAA_C	5	2	20	2

Fig. 2 Classification outcomes per assay of the multiple systems atrophy (MSA) subgroup. Graph showing the diagnostic classification assigned by each assay (SPB-SAA_A, SPB-SAA _B, PIPES-SAA_A, PIPES-SAA _C) for each individual patient (columns), where SPB-SAA refers to sodium phosphate buffer seed amplification assay and PIPES-SAA refers to piperazine-*N*,*N*′-bis(2-ethanesulfonic acid) seed amplification assay. Colors represent the classification outcome per assay: synSAA+ type 1, synSAA+ type 2, synSAA−, or inconclusive. In SPB-SAA_A, an "X" marks the samples that required retesting due to an initial inconclusive result. Lower row shows the concordance rate between sites (number of concordant results per 4 assays). At the bottom, a summary table reports the total number of patients classified into each category by assay

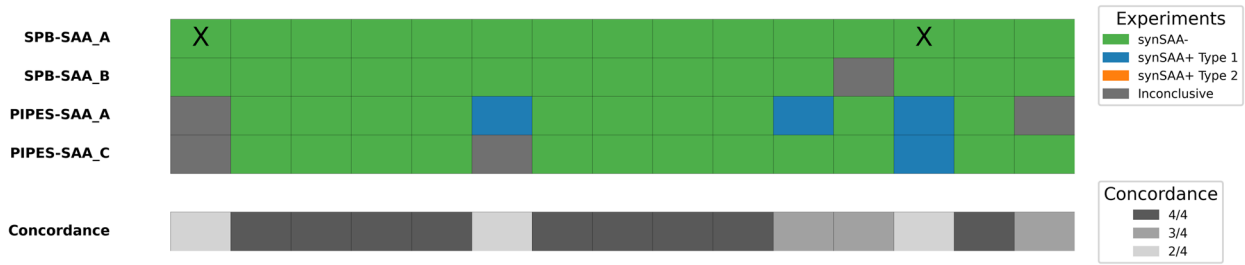

	synSAA-	synSAA+ Type 1	synSAA+ Type 2	Inconclusive
SPB-SAA_A	15	0	0	0
SPB-SAA_B	14	0	0	1
PIPES-SAA_A	10	3	0	2
PIPES-SAA_C	12	1	0	2

Fig. 3 Classification outcomes per assay of the control subgroup. Graph showing the diagnostic classification assigned by each assay (SPB-SAA_A, SPB-SAA _B, PIPES-SAA_A, PIPES-SAA _C) for each individual patient (columns), where SPB-SAA refers to sodium phosphate buffer seed amplification assay and PIPES-SAA refers to piperazine-*N*,*N*′-bis(2-ethanesulfonic acid) seed amplification assay. Colors represent the classification outcome per assay: synSAA+ type 1, synSAA+ type 2, synSAA−, or inconclusive. In SPB-SAA_A, an "X" marks the samples that required retesting due to an initial inconclusive result. Lower row shows the concordance rate between sites (number of concordant results per 4 assays). At the bottom, a summary table reports the total number of patients classified into each category by assay

identical classification performance. SPB-SAA and PIPES-SAA overlapped in eight of the synSAA+ cases (Fig. 1). Importantly, all synSAA+ PD/DLB* presented type1 syn-seeds at both sites. Concordance across assays was very high, where only two patients were classified differently between the two synSAA protocols. Clinical details of the two discordant PD cases, including age at onset, disease duration, and clinical scales, are provided in supplementary Table S2.

SPB-SAA_A and SPB-SAA_B detected seeding activity in 2 of the 29 CSF samples from clinically diagnosed patients with MSA. SPB-SAA_B classified one sample as inconclusive, and SPB-SAA_A had to retest three samples with inconclusive status. The fluorescence amplification pattern of these samples was indistinguishable from the synSAA+ PD/DLB* cases. In contrast, type 2 syn-seeds were respectively detected in 19 and 21 of the 29 MSA CSF samples by PIPES-SAA_A and PIPES-SAA_C, with 18 samples overlapping between sites (Fig. 2). There was no CSF volume for retests with the PIPES-SAA protocol, and PIPES-SAA_A and PIPES-SAA_C had one and two inconclusive samples, respectively. Two MSA CSF samples were classified as synSAA+ type 1 in both sites, suggesting underlying Lewy body disease. Interestingly, these were the two CSF samples that showed seeding activity by SPB-SAA. Clinical details of these cases, including age at onset, disease duration, and clinical scales, are provided in supplementary Table S2. Considering all MSA samples and assays, inter-site agreement was high, but, as expected, inter-assay agreement was low, given that SPB-SAA does not detect synuclein seeding activity in MSA (Fig. 2).

In the neurology ward control group, 15 and 14 of the 15 CSF samples were classified as synSAA– by SPB-SAA_A and SPB-SAA_B, respectively (Fig. 3). SPB-SAA_B reported one control as inconclusive, and there was no volume available for retest; remeasurement had to be performed for three inconclusive samples in SPB-SAA_A. PIPES-SAA_A classified 10 CSF samples as synSAA–, three as synSAA+ type 1, and two inconclusive that were not retested because of lack of sample. PIPES-SAA_C classified 12 CSF samples as synSAA–, one as synSAA+ type 1, and two inconclusive that were not retested because of lack of volume. Interestingly, one inconclusive and one synSAA+ type 1 sample had matching results between sites using the PIPES-SAA protocol, while one PIPES-SAA_A synSAA+ type 1 sample was inconclusive at site C (not retested). Importantly, no controls were classified as synSAA+ type 2 by either PIPES-SAA site. Considering all control samples and assays, inter-assay concordance was high and inter-site agreement was higher for the SPB-SAA protocol.

Sensitivity and Specificity for synSAA+ MSA Cases

Sensitivity for synSAA+ MSA cases was calculated using clinical diagnosis as the gold standard for the PIPES-SAA protocol, but not for the SPB-SAA protocol, since it was not possible to differentiate MSA and control groups with this protocol (Fig. 4). Sensitivity and specificity were calculated excluding individuals with an inconclusive classification. For detection of synuclein seeds in MSA, PIPES-SAA_A demonstrated a sensitivity of 75.0% and a specificity of 76.9%, while

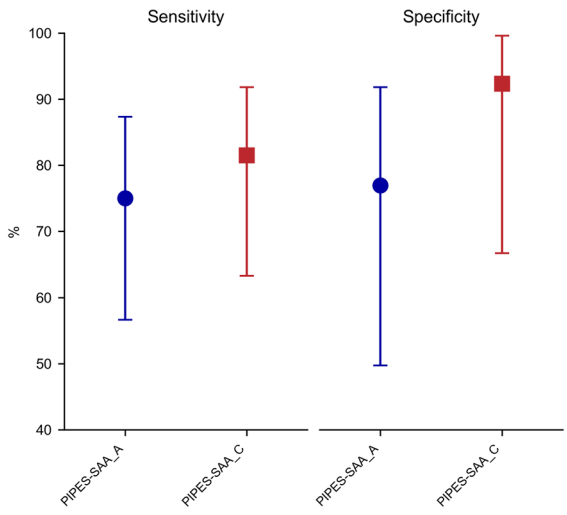

Fig. 4 Sensitivity and specificity of PIPES-SAA assays for multiple systems atrophy (MSA) detection, where PIPES-SAA refers to piperazine-*N*,*N*′-bis(2-ethanesulfonic acid) seed amplification assay. Sensitivity and specificity for detecting synuclein seeds in MSA using the PIPES-SAA_A and PIPES-SAA_C assays. Data are represented as percentages with 95% confidence intervals indicated by error bars

PIPES-SAA_C showed a sensitivity of 81.4% and a specificity of 92.3%.

Inter-assay Concordance

We assessed inter-assay concordance to evaluate the technical reproducibility across sites and protocols. Table 3 summarizes concordance rates for each comparison overall and within diagnostic subgroups, excluding samples with inconclusive results in any assay.

PIPES-SAA_A and PIPES-SAA_C demonstrated an overall concordance of 95%, with subgroup rates of 100% for PD/DLB*, 93% for MSA, and 92% for controls. The overall Fleiss' kappa for PIPES-SAA protocol was 0.913 ($p < 1.0 \times 10^{-5}$). Subgroup kappa values were high as well: 1.00 ($p = 6.0 \times 10^{-5}$) for PD/DLB*, 0.83 ($p < 1.0 \times 10^{-5}$) for MSA, and 0.61 ($p = 0.0030$) for controls. SPB-SAA_A and SPB-SAA_B demonstrated 100% agreement for overall concordance and for within diagnostic subgroups. The overall Fleiss' kappa for SPB-SAA was 1.00 ($p < 1.0 \times 10^{-5}$).

When comparing mean results across sites between protocols, the overall concordance showed, as expected, only a fair agreement overall (59%), with a Fleiss' kappa of 0.23 ($p = 0.0258$), given the different outcomes between the two assays in MSA. In contrast, concordance for PD/DLB* was high at 88% (kappa = 0.74, $p = 0.0026$), indicating substantial agreement.

For the control group, concordance between PIPES-SAA and SPB-SAA protocols was 86%, though Fleiss' kappa was negative (− 0.10, $p = 0.5640$). This likely reflects the high prevalence of synSAA− classifications across both assays, which inflates raw concordance while limiting kappa's sensitivity as a result of the lack of category variability in this subgroup. Similarly, no kappa value was computed for the control group between the SPB-SAA A and B because of the absence of classification variability, since all controls were uniformly classified as synSAA−, preventing the calculation of inter-rater agreement beyond perfect concordance.

After the first testing round, seven samples in SPB-SAA_A required repeat testing, after which all were classified conclusively. In other sites, limited CSF volume did not permit repeat testing for the samples with an inconclusive status. Thus, the frequency of inconclusive results per

Table 3 Inter-assay concordance rates, Fleiss' kappa values, and associated *p* values across diagnostic subgroups

Comparison	PD/DLB*	PD/DLB* kappa (*p* value)	MSA	MSA kappa (*p* value)	Controls	Controls kappa (*p* value)	Overall	Overall kappa (*p* value)
PIPES-SAA_A vs PIPES-SAA_C	100%	1.00 (6.0×10^{-5})	93%	0.83 ($< 1.0 \times 10^{-5}$)	92%	0.61 (0.0030)	95%	0.913 ($< 1 \times 10^{-5}$)
SPB-SAA_A vs SPB-SAA_B	100%	1.00 (6.0×10^{-5})	100%	1.00 ($< 1.0 \times 10^{-5}$)	100%	NA	100%	1.00 ($< 1 \times 10^{-5}$)
PIPES-SAA vs SPB-SAA	88%	0.74 (0.0026)	31%	− 0.33 (0.0233)	86%	− 0.10 (0.5640)	59%	0.230 (0.0258)

Percentage of concordant classifications between assays overall and within each diagnostic subgroup: PD/DLB*, MSA, and controls. Fleiss' kappa coefficient with corresponding *p* values are reported to quantify agreement beyond chance. A negative kappa value indicates agreement lower than expected by chance. Individuals with inconclusive classification in any of the compared assays were excluded from the analysis

PD Parkinson's disease, *DLB* dementia with Lewy bodies, *MSA* multiple systems atrophy, *SPB-SAA* sodium phosphate buffer seed amplification assay, *PIPES-SAA* piperazine-*N*,*N*′-bis(2-ethanesulfonic acid) seed amplification assay

assay was as follows: PIPES-SAA_A, 5.0%; PIPES-SAA_C, 6.67%; SPB-SAA_A, 0%; and SPB-SAA_B, 3.33%.

DISCUSSION

This systematic 2 × 2 comparative study replicates previous studies showing that different optimized synSAA protocols can produce similar results for PD/DLB* and control samples, but not for MSA [18, 19, 25]. As expected, there was low agreement between protocols as a result of the MSA group, and high agreement within protocols, with SPB-SAA and PIPES-SAA reaching kappa values of 1 and 0.913. It is important to mention that the PD/DLB* group was preselected using the SPB-SAA protocol, which could have exacerbated the agreement between sites.

The main difference between these protocols was the detection of seeding activity in the MSA group, with concordance reaching only 31%. While the SPB-SAA protocol did not detect type 2 synuclein seeds, the PIPES-SAA sites reached 75% and 81% sensitivity using clinical diagnosis as the gold standard. The two MSA samples that were found synSAA+ by SPB-SAA were identified as synSAA+ type 1 by the PIPES-SAA protocol. Since previous studies using brain samples and pathology have confirmed that CSF samples demonstrate low sensitivity for MSA using SPB-SAA, and high sensitivity and specificity of the PIPES-SAA protocol for type 1 and type 2 synuclein seeds [14, 18], these two cases are most likely PD cases misdiagnosed as MSA. The PIPES-SAA protocol achieved sensitivities for synSAA+ MSA cases similar to those reported previously [18, 26]. While PIPES-SAA specificity was high, occasional false positives in controls (mainly with type 1 synuclein seeds) led to reduced specificity in PIPES-SAA_A (76.92%) compared to PIPES-SAA_C (92.31%). However, it is known that synSAA positivity increases with age and that many clinical presentations have mixed underlying pathologies; thus, there is a possibility that neurology ward controls with synSAA+ results might not be false positives.

The biological basis for the differential detection capabilities of the assays remains incompletely understood. Examination of the type 1 and type 2 synuclein amplification curves of the PIPES-SAA (Fig. S1) reveals that both reach a fluorescence plateau, although at different RFU values, which forms the basis of their classification. Given the near 100% conversion rate of the substrate and the negligible concentration of monomeric and misfolded synuclein in CSF, the difference in fluorescence plateau is not explained by a difference in the quantity of aggregates. The difference in fluorescence could be explained by differences in fibril ultrastructure or the folding of synuclein in the type 1 and type 2 amplified synuclein seeds. Different structures could have different ThT bindings pockets, which could change the binding capacity of ThT to the aggregate and/or change the ThT fluorescence intensity by increasing/reducing fluorescence quenching, while different ultrastructure could cause light-scattering and/or block ThT binding pockets. Direct structural and kinetic analysis will be required to clarify the precise basis of these divergent profiles [27]. This hypothesis aligns with the recent structural studies showing distinct ultrastructural properties of αSyn strains in PD/DLB versus MSA [17, 27, 28]. Consequently, the differential detection of MSA seeding activity by PIPES-SAA compared to SPB-SAA may be explained the chemical and physical reaction conditions in PIPES-SAA (e.g., buffer composition, bead type, shaking pattern), which may better support the amplification of the conformers found in MSA.

This study has several limitations. First, the PD/DLB cohort was methodologically enriched for synSAA– cases, which precludes valid sensitivity estimates for PD/DLB detection in a real-world setting. Second, the cohort size was modest, especially for MSA and controls, which may have impacted sensitivity estimates and kappa stability, as reflected by the wide confidence intervals observed in Fig. 4. Third, the control cases had neurological symptoms as they were not healthy controls, which complicates the interpretation of "false positives". Longitudinal follow-up of these control individuals would be valuable to determine whether synSAA positive controls go on to develop a clinically overt synucleinopathy. Furthermore, systematic functional neuroimaging such as DAT-SPECT or PET

examinations were not performed in all participants; instead, MRI and CSF neurofilament light chain (NfL) levels were used as supporting diagnostic tools, which is consistent with current clinical practice but represents an additional limitation in terms of absolute diagnostic certainty. Lastly, while we quantified reproducibility using concordance and Fleiss' kappa, further multicenter validations with larger and clinically representative cohorts are needed to confirm generalizability.

CONCLUSIONS

Our systematic comparison demonstrates the high technical reproducibility of synSAAs across sites and protocols, while reinforcing the distinct detection profiles of PIPES-SAA and SPB-SAA. Together, these results help refine the positioning of SAAs within the diagnostic landscape of synucleinopathies and highlight the need for larger multicenter studies, continued protocol optimization, and deeper biological characterization of αSyn strains to improve diagnostic sensitivity and specificity.

ACKNOWLEDGEMENTS

The authors wish to thank all patients and their families for participating in this study. We also thank the physicians and nurses involved in performing lumbar punctures and supporting sample logistics, whose contributions were essential for this work. We thank Madeleine Wacker, MSc, and Benjamin Riebenbauer for coordinating the aliquoting and distribution of the samples across centers. We acknowledge support from the Open Access Publication Fund of the University of Tuebingen. Samples were obtained from the Neurobiobank of the University of Tuebingen, Germany (https://www.hih-tuebingen.de/en/about-us/core-facilities/biobank/). This biobank is supported by the local University, the Hertie institute, and the DZNE.

Medical Writing/Editorial Assistance. No medical writing or editorial assistance beyond AI-assisted copy editing was used in the preparation of this manuscript.

Author Contributions. Conception and design of the study: Thomas Gasser, Kathrin Brockmann, Matthis Synofzik, David Mengel. Execution of the study: Kathrin Brockmann, Matthis Synofzik, David Mengel (Clinical examination and lumbar puncture); Roger Plaza-Clar, Maximilian Weber, Christian Deuschle, Marcello Rossi, Angela Mammana (SPB-SAA), Vaibhavi Kadam, Luis Concha-Marambio, Yihua Ma, Carly M Farris (PIPES-SAA). Sample acquisition and handling: Christian Deuschle. Data analysis: Roger Plaza-Clar, Maximilian Weber, Vaibhavi Kadam, Luis Concha-Marambio, Yihua Ma, Carly M Farris, David Mengel, Marcello Rossi, Angela Mammana, Piero Parchi, Matthis Synofzik, Kathrin Brockmann, Thomas Gasser. Statistical analysis: Roger Plaza-Clar, Maximilian Weber, Vaibhavi Kadam. Data interpretation: Roger Plaza-Clar, Maximilian Weber, Vaibhavi Kadam, Matthis Synofzik, Kathrin Brockmann, Thomas Gasser. Writing of the original draft: Roger Plaza-Clar. Writing, reviewing and editing: Roger Plaza-Clar, Maximilian Weber, Vaibhavi Kadam, Matthis Synofzik, Kathrin Brockmann, Thomas Gasser. Critical review of the manuscript: Roger Plaza-Clar, Maximilian Weber, Vaibhavi Kadam, Christian Deuschle, Luis Concha-Marambio, Yihua Ma, Carly M Farris, David Mengel, Marcello Rossi, Angela Mammana, Piero Parchi, Matthis Synofzik, Kathrin Brockmann, Thomas Gasser. All authors read and approved the final manuscript.

Funding. Funding was provided in part by the Michael J Fox Foundation (Grant-ID MJFF-022411). This work was supported by the Clinician Scientist programme "PRECISE.net" funded by the Else Kröner-Fresenius-Stiftung (to Matthis Synofzik and David Mengel), and by the European Union, project European Rare Disease Research Alliance (ERDERA), GA no. 101156595, funded under call HORIZON-HLTH-2023-DISEASE-07 (to Matthis Synofzik). The study was supported in part by the Ministero della Salute, Italy (Grant RF-2021-12374386). The Rapid Service Fee was funded in part by the Open Access

Publication Fund of the University of Tübingen and in part by Thomas Gasser.

Data Availability. The anonymized datasets generated during and/or analyzed during the current study are available upon reasonable request to: rogerplazac@gmail.com.

Declarations

Conflict of Interest. Thomas Gasser has received research support from the German Research Foundation (DFG), the German Ministry of Research (BMBF), the European Commission, the Michael J Fox Foundation, Chem Div. Inc, and the Charitable Hertie Foundation. He has received speaker's honoraria from UCB Pharma, Novartis, Sanofi, BIAL and MedUpdate and consulting fees from Bayer AG, Blue Rock Therapeutics and Coave Therapeutics, Ono Pharmaceutical, Lilly Deutschland GmbH, Roche Pharma AG, BIAL, Biogen MA Inc. and SciNeuro Therapeutics. Kathrin Brockmann has received research funding from the Michael J. Fox Foundation for Parkinson's Research, the German Society for Parkinson DPG, the Health Forum Baden Wuerttemberg, the Else Kröner-Fresenius-Stiftung, the University of Tuebingen, and from the German Research Foundation DFG. Kathrin Brockmann is a consultant for F. Hoffmann-La Roche Ltd., Vanqua Bio, and the Michael J. Fox Foundation for Parkinson's Research and has received speaker honoraria from Abbvie, Lundbeck, UCB and Zambon. Matthis Synofzik has received consultancy honoraria from UCB, Prevail, Orphazyme, Biogen, Servier, Reata, GenOrph, AviadoBio, Biohaven, Zevra, Lilly, Quince, Neurocrine, Insmed, and Solaxa, all unrelated to the present manuscript. Luis Concha-Marambio, Yihua Ma, and Carly M Farris are employees of Amprion and declares employee stock option ownership and invention of patents related to SAA technology assigned to Amprion. Roger Plaza-Clar, Maximilian Weber, Vaibhavi Kadam, Christian Deuschle, David Mengel, Marcello Rossi, Angela Mammana, Piero Parchi, have nothing to disclose.

Ethical Approval. The study was approved by the Ethics Committee of the University of Tuebingen (353/2022BO2). All participants gave written informed consent for participation in the study and for the use and publication of their anonymized data. This study was conducted in accordance with the principles of the Declaration of Helsinki.

REFERENCES

1. Goedert M, Spillantini MG, Del Tredici K, Braak H. 100 years of Lewy pathology. Nat Rev Neurol. 2013. https://doi.org/10.1038/nrneurol.2012.242.

2. Levin J, Kurz A, Arzberger T, Giese A, Höglinger GU. The differential diagnosis and treatment of atypical parkinsonism. Dtsch Arztebl Int. 2016;113(5):61–9. https://doi.org/10.3238/arztebl.2016.0061.

3. Koga S, Sekiya H, Kondru N, Ross OA, Dickson DW. Neuropathology and molecular diagnosis of synucleinopathies. Mol Neurodegener. 2021. https://doi.org/10.1186/s13024-021-00501-z.

4. Schweighauser M, Shi Y, Tarutani A, et al. Structures of α-synuclein filaments from multiple system atrophy. Nature. 2020. https://doi.org/10.1038/s41586-020-2317-6.

5. Yang Y, Shi Y, Schweighauser M, et al. Structures of α-synuclein filaments from human brains with

Lewy pathology. Nature. 2022. https://doi.org/10.1038/s41586-022-05319-3.

6. Van der Perren A, Gelders G, Fenyi A, et al. The structural differences between patient-derived α-synuclein strains dictate characteristics of Parkinson's disease, multiple system atrophy and dementia with Lewy bodies. Acta Neuropathol. 2020. https://doi.org/10.1007/s00401-020-02157-3.

7. Peng C, Gathagan RJ, Covell DJ, et al. Cellular milieu imparts distinct pathological α-synuclein strains in α-synucleinopathies. Nature. 2018. https://doi.org/10.1038/s41586-018-0104-4.

8. Adler CH, Beach TG, Hentz JG, et al. Low clinical diagnostic accuracy of early vs advanced Parkinson disease: clinicopathologic study. Neurology. 2014. https://doi.org/10.1212/WNL.0000000000000641.

9. Keener AM, Bordelon YM. Parkinsonism. Semin Neurol. 2016;36(4):330–4. https://doi.org/10.1055/s-0036-1585097.

10. Moda F, Gambetti P, Notari S, et al. Prions in the urine of patients with variant Creutzfeldt–Jakob disease. N Engl J Med. 2014. https://doi.org/10.1056/nejmoa1404401.

11. Atarashi R, Wilham JM, Christensen L, et al. Simplified ultrasensitive prion detection by recombinant PrP conversion with shaking. Nat Methods. 2008. https://doi.org/10.1038/nmeth0308-211.

12. Groveman BR, Orrù CD, Hughson AG, et al. Rapid and ultra-sensitive quantitation of disease-associated α-synuclein seeds in brain and cerebrospinal fluid by αSyn RT-QuIC. Acta Neuropathol Commun. 2018. https://doi.org/10.1186/s40478-018-0508-2.

13. Russo MJ, Orru CD, Concha-Marambio L, et al. High diagnostic performance of independent alpha-synuclein seed amplification assays for detection of early Parkinson's disease. Acta Neuropathol Commun. 2021. https://doi.org/10.1186/s40478-021-01282-8.

14. Rossi M, Candelise N, Baiardi S, et al. Ultrasensitive RT-QuIC assay with high sensitivity and specificity for Lewy body-associated synucleinopathies. Acta Neuropathol. 2020. https://doi.org/10.1007/s00401-020-02160-8.

15. Arnold MR, Coughlin DG, Brumbach BH, et al. α-Synuclein seed amplification in CSF and brain from patients with different brain distributions of pathological α-synuclein in the context of co-pathology and non-LBD diagnoses. Ann Neurol. 2022. https://doi.org/10.1002/ana.26453.

16. Siderowf A, Concha-Marambio L, Lafontant DE, et al. Assessment of heterogeneity among participants in the Parkinson's Progression Markers Initiative cohort using α-synuclein seed amplification: a cross-sectional study. Lancet Neurol. 2023. https://doi.org/10.1016/S1474-4422(23)00109-6.

17. Shahnawaz M, Mukherjee A, Pritzkow S, et al. Discriminating α-synuclein strains in Parkinson's disease and multiple system atrophy. Nature. 2020. https://doi.org/10.1038/s41586-020-1984-7.

18. Ma Y, Farris CM, Weber S, et al. Sensitivity and specificity of a seed amplification assay for diagnosis of multiple system atrophy: a multicentre cohort study. Lancet Neurol. 2024;23(12):1225–37. https://doi.org/10.1016/S1474-4422(24)00395-8.

19. Rossi M, Farris CM, Baiardi S, et al. Comparison of two α-synuclein seed amplification assays for discrimination of Parkinson disease and atypical parkinsonism. Mov Disord. 2025. https://doi.org/10.1002/mds.70017.

20. Litvan I, Bhatia KP, Burn DJ, et al. SIC task force appraisal of clinical diagnostic criteria for parkinsonian disorders. Mov Disord. 2003. https://doi.org/10.1002/mds.10459.

21. McKeith IG, Boeve BF, Dickson DW, et al. Diagnosis and management of dementia with Lewy bodies: fourth consensus report of the DLB Consortium. Neurology. 2017;89(1):88–100.

22. Gilman S, Wenning GK, Low PA, et al. Second consensus statement on the diagnosis of multiple system atrophy. Neurology. 2008. https://doi.org/10.1212/01.wnl.0000324625.00404.15.

23. Mammana A, Baiardi S, Rossi M, et al. Improving protocols for α-synuclein seed amplification assays: analysis of preanalytical and analytical variables and identification of candidate parameters for seed quantification. Clin Chem Lab Med. 2024. https://doi.org/10.1515/cclm-2023-1472.

24. Brockmann K, Quadalti C, Lerche S, et al. Association between CSF alpha-synuclein seeding activity and genetic status in Parkinson's disease and dementia with Lewy bodies. Acta Neuropathol Commun. 2021. https://doi.org/10.1186/s40478-021-01276-6.

25. Kang UJ, Boehme AK, Fairfoul G, et al. Comparative study of cerebrospinal fluid α-synuclein seeding aggregation assays for diagnosis of Parkinson's disease. Mov Disord. 2019. https://doi.org/10.1002/mds.27646.

26. Concha-Marambio L, Pritzkow S, Shahnawaz M, Farris CM, Soto C. Seed amplification assay for the detection of pathologic alpha-synuclein aggregates

in cerebrospinal fluid. Nat Protoc. 2023. https://doi.org/10.1038/s41596-022-00787-3.

27. Enomoto M, Martinez-Valbuena I, Forrest SL, et al. Lewy-MSA hybrid fold drives distinct neuronal α-synuclein pathology. Commun Biol. 2025. https://doi.org/10.1038/s42003-025-08355-7.

28. Tarutani A, Hasegawa M. Ultrastructures of α-synuclein filaments in synucleinopathy brains and experimental models. J Mov Disord. 2024. https://doi.org/10.14802/jmd.23213.